

## Nonequilibrium Quantum Magnetism in a Dipolar Lattice Gas

A. de Paz,<sup>1,2</sup> A. Sharma,<sup>2,1</sup> A. Chotia,<sup>2,1</sup> E. Maréchal,<sup>2,1</sup> J. H. Huckans,<sup>4,1</sup> P. Pedri,<sup>1,2</sup> L. Santos,<sup>3</sup> O. Gorceix,<sup>1,2</sup>  
L. Vernac,<sup>1,2,\*</sup> and B. Laburthe-Tolra<sup>2,1</sup>

<sup>1</sup>Université Paris 13, Sorbonne Paris Cité, Laboratoire de Physique des Lasers, F-93430 Villetaneuse, France

<sup>2</sup>CNRS, UMR 7538, LPL, F-93430 Villetaneuse, France

<sup>3</sup>Institut für Theoretische Physik, Leibniz Universität Hannover, Appelstraße 2, DE-30167 Hannover, Germany

<sup>4</sup>Department of Physics and Engineering Technology, Bloomsburg University of Pennsylvania, Bloomsburg, Pennsylvania 17815, USA

(Received 12 July 2013; revised manuscript received 6 September 2013; published 30 October 2013)

We report on the realization of quantum magnetism using a degenerate dipolar gas in an optical lattice. Our system implements a lattice model resembling the celebrated  $t$ - $J$  model. It is characterized by a nonequilibrium spinor dynamics resulting from intersite Heisenberg-like spin-spin interactions provided by nonlocal dipole-dipole interactions. Moreover, due to its large spin, our chromium lattice gases constitute an excellent environment for the study of quantum magnetism of high-spin systems, as illustrated by the complex spin dynamics observed for doubly occupied sites.

DOI: [10.1103/PhysRevLett.111.185305](https://doi.org/10.1103/PhysRevLett.111.185305)

PACS numbers: 67.85.-d, 03.75.Mn, 05.30.Jp, 05.70.Ln

The study of quantum magnetism is of utmost importance for the understanding of a variety of modern materials with strong correlations [1]. Cold atoms loaded in periodic optical potentials provide a new platform for the investigation of quantum magnetism that presents several important and interesting features, such as the absence of unwanted disorder, and the possibility to tune the interparticle interactions [2]. This results in a well-defined Hamiltonian correctly describing the system. For this reason, there has been in recent years huge interest towards using atoms in optical lattices as quantum simulators for various theoretically intractable many-body problems [3], relevant for phenomena such as high- $T_c$  superconductivity.

Dilute atomic gases possess specific properties that result in qualitatively novel physics compared to that of electrons in solids. In particular, atoms may carry a larger spin  $s > 1/2$  provided by their internal structure, which results in an exceedingly rich phenomenology [4,5]. In particular, atomic gases in optical lattices allow for the realization of quantum magnetism with  $s > 1/2$ , which results in a wealth of novel quantum phases, such as spin nematics [6], color superfluidity [7], or chiral spin liquids [8].

Dipolar gases, which may be realized either with magnetic atoms [9–13] or with polar molecules [14–17], open fascinating possibilities for the engineering of models of quantum magnetism [18–23]. In nondipolar gases, contact interactions do not couple atoms belonging to different lattice sites, and, hence, an effective intersite spin exchange can only result from tunneling-assisted processes. Effective exchange can result from superexchange interactions scaling as  $J^2/U$  [24,25], or, in the case of effective spin models in tilted lattices, from direct tunneling  $J$  [26,27]. In contrast, the long range dipole-dipole interactions (DDIs) provide a direct intersite spin-spin coupling [28,29] which hence becomes independent of tunneling. Moreover, relatively large intersite spin coupling ( $\sim 20$  Hz for the case of our

chromium experiments) eases the constraints of studying quantum magnetism within the time scale set by the coherence time.

This Letter pioneers, to the best of our knowledge, the experimental realization of quantum magnetism with a degenerate dipolar gas in an optical lattice. We study the particular case of  $^{52}\text{Cr}$  bosons, a system that possesses not only unusually strong magnetic DDIs, but a large spin ( $s = 3$ ) as well, and thus allows for the investigation of the rich physics expected for high-spin lattice gases. Our experimental results on spin dynamics reveal spin exchange between different lattice sites mediated by the DDIs. We first explore the case with maximally one atom per site, where spinor dynamics is solely provided by intersite DDIs, and may be well described by a model resembling the well known  $t$ - $J$  Hamiltonian, a fundamental model of quantum magnetism [1]. We then investigate the scenario where two atoms may occupy the same site, in which the interplay between contact and dipolar interactions leads to a rich spin-exchange physics characterized by two markedly different coherent spin oscillations. Whereas on-site contact interactions lead to fast spin oscillations at short time scales, coherent oscillations of a much lower frequency are observed at longer times. We show that the latter disappear when a magnetic field gradient is applied, hence demonstrating that slow coherent oscillations result from DDIs between doubly occupied sites.

The DDI between two atoms having a dimensionless spin  $\mathbf{S}_i$  is described by the Hamiltonian

$$\hat{H}_d = d^2 \frac{\hat{\mathbf{S}}_1 \cdot \hat{\mathbf{S}}_2 - 3(\hat{\mathbf{S}}_1 \cdot \hat{\mathbf{r}})(\hat{\mathbf{S}}_2 \cdot \hat{\mathbf{r}})}{4\pi r^3}, \quad (1)$$

where  $d^2 = \mu_0(g\mu_B)^2$  ( $\mu_0$  being the magnetic permeability of vacuum,  $g$  the Lande factor, and  $\mu_B$  the Bohr magneton), and  $\hat{\mathbf{r}} = \mathbf{r}/r$  with  $\mathbf{r} = \mathbf{r}_1 - \mathbf{r}_2$  the interatomic separation. The Hamiltonian (1) includes magnetization

changing terms, which may crucially modify the spinor physics by introducing free magnetization [30], and an intrinsic spin-orbit coupling [31,32]. However, we have recently shown that these terms have a resonant character in a 3D lattice, and therefore are strongly suppressed at a low enough magnetic field  $\mathbf{B}$  [33]. In this case, considered throughout this Letter, the spin projection along the  $\mathbf{B}$  field is conserved, and hence only Ising and exchange terms play a role. As a result, the Hamiltonian of Eq. (1) can be reduced [34] to an effective XXZ spin Hamiltonian [1]:

$$\hat{H}_d^{\text{eff}} = \frac{d^2}{4\pi r^3} \left(1 - 3\frac{z^2}{r^2}\right) \left(\hat{S}_{1z}\hat{S}_{2z} - \frac{1}{4}(\hat{S}_1^+\hat{S}_2^- + \hat{S}_1^-\hat{S}_2^+)\right), \quad (2)$$

with  $z$  the relative coordinate along the  $\mathbf{B}$  field. Our experimental results described below reveal the spinor dynamics induced by intersite spin-spin interactions of this Heisenberg-like Hamiltonian: a chromium gas loaded in a 3D lattice provides an interesting platform for the analysis of quantum magnetism.

In our experiment, we first create a chromium Bose-Einstein condensate in a crossed-beam optical dipole trap as described in Ref. [10]. The condensate, comprising about  $10^4$  atoms polarized in the absolute ground Zeeman state  $m_s = -3$ , is confined at the bottom of a harmonic trap with frequencies  $(\omega_x, \omega_y, \omega_z) = 2\pi \times (400, 550, 300)$  Hz, within a magnetic field of  $B = 10$  mG. The Bose-Einstein condensate is loaded adiabatically in a 3D optical lattice, generated using 4 W of a single-mode laser with wavelength  $\lambda = 532$  nm. The five-beam architecture of our anisotropic lattice is described in [33]. It consists of a rectangular lattice of periodicity  $\lambda/2 \times (1, 1/\sin(\pi/8), 1/\cos(\pi/8))$  along the  $x$ ,  $y$ , and  $z$  directions. The lattice depths in each direction are calibrated using Kapitza-Dirac diffraction [35] for pairs of beams, leading to a maximum of  $30 E_R$  (with  $E_R = \hbar^2/2m\lambda^2$  the recoil energy). In this Letter (unless stated otherwise) we work at this lattice depth, which corresponds to lattice band gaps  $(\omega_x^L, \omega_y^L, \omega_z^L) = 2\pi \times (100, 55, 170)$  kHz. For our experimental parameters, the predicted ground state is then a Mott-insulator state characterized by a central region with double occupancy surrounded by a single occupancy shell. The superfluid to Mott insulator transition is reached at about  $12 E_R$  [36] (see Supplemental Material, part S1 [37]). The lattice band gaps are much larger than all other energy scales in the system (interactions, temperature, Zeeman shifts), and, hence, the atoms remain confined to the lowest energy band of the lattice.

In the experiments described in this Letter, we initiate spin dynamics by transferring atoms to  $m_s = -2$  (see Supplemental Material, part S2 [37]), with a typical efficiency of 70%, and up to 80%. We then let the spin populations evolve and perform a Stern-Gerlach analysis after a given time  $t$  to measure the different spin populations.

To demonstrate the existence of intersite spin exchange, we first selectively remove atoms which share the same site (see Ref. [33] and Supplemental Material, part S3 [37]). After this preparation, the system consists of a shell of about 4000 singly occupied sites close to unit filling. Then atoms are transferred to  $m_s = -2$ . Populations in states  $m_s = -3, -2, -1, 0$  evolve as a function of time in a typical time scale of 10 ms while the magnetization remains constant within error bars. To maximize the signal-to-noise ratio, we plot the ratio of populations in  $m_s = -3$  and  $m_s = -2$  as a function of  $t$  in Fig. 1. Given that no site contains more than one atom, the observed spin dynamics is necessarily the product of an intersite spin exchange process. In particular, we stress that at our lattice depth, tunneling producing double occupancy is strongly suppressed by the on-site contact interactions ( $\approx 10$  kHz). As a result, any associated spin exchange process has a rate below 0.1 Hz (set by superexchange interactions [25]), which is incompatible with our observations. The spin dynamics shown in Fig. 1 is therefore a direct demonstration of dipolar intersite spin exchange.

The spin dynamics of the singlon gas may be well understood from a 2D  $t$ - $J$ -like Hamiltonian [1]. The 2D

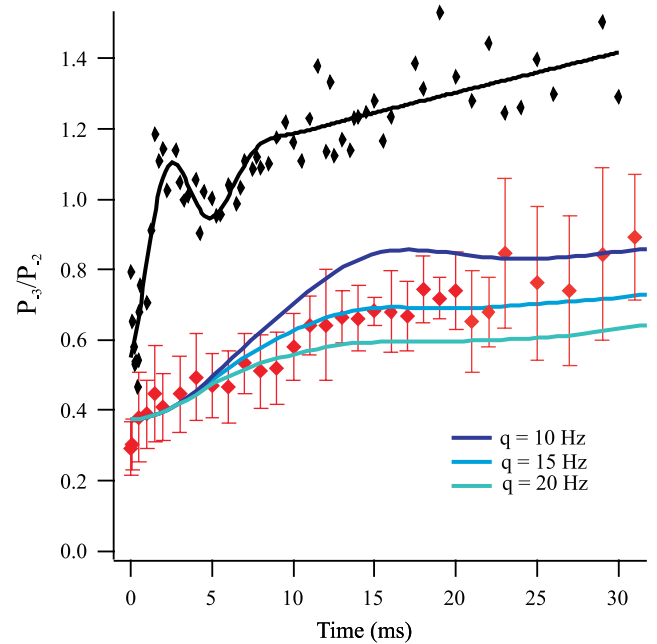


FIG. 1 (color online). Long term spin dynamics. The ratio between two Zeeman spin components is plotted as a function of time. For this specific data, the lattice depth corresponds to lattice band gaps of  $(\omega_x^L, \omega_y^L, \omega_z^L) = 2\pi \times (130, 55, 150)$  kHz. Experimental results are shown for singlons only (red diamonds) and for singlons plus doublons (black diamonds). Error bars show statistical uncertainties. The two dynamics show the same trend after 10 ms. The black line is a fit to the data (damped sinusoid + exponential) to guide the eye. The colored lines are results of our simulation for spins 3 on a  $3 \times 3$  plaquette, for three different quadratic effects, and tunneling rates  $J_{(x,z)} = (11, 13)$  Hz (deduced from lattice calibrations).

assumption is well justified due to the anisotropy of the lattice spacing, which is basically equal along  $x$  and  $z$  but approximately 3 times larger along  $y$ . The  $t$ - $J$ -like Hamiltonian acquires the form

$$\hat{H} = - \sum_{\langle i,j \rangle, m_s} J_{i,j} \hat{b}_{i,m_s}^\dagger \hat{b}_{j,m_s} + q \sum_{j,m_s} m_s^2 \hat{n}_{j,m_s} + \sum_{i,j} V_{i,j} \left( \hat{S}_i^z \hat{S}_j^z - \frac{1}{4} (\hat{S}_i^+ \hat{S}_j^- + \hat{S}_i^- \hat{S}_j^+) \right). \quad (3)$$

In Eq. (3),  $\langle \cdot \cdot \cdot \rangle$  denotes nearest neighbors,  $\hat{b}_j$  and  $\hat{b}_j^\dagger$  the bosonic annihilation and creation operators of particles at site  $j = (j_x, j_z)$  with spin projection  $m_s$ ,  $\hat{n}_{j,m_s} = \hat{b}_{j,m_s}^\dagger \hat{b}_{j,m_s}$ , and  $\hat{n}_j = \sum_{m_s} \hat{n}_{j,m_s}$ . The hard-core constraint,  $n_j = 0, 1$ , is justified by the large on-site contact interaction associated with doubly occupied sites. Hopping, characterized by the rate  $J_{i,j}$ , is possible, however, due to the presence of residual empty sites. Estimated tunneling rates along the  $(x, z)$  directions are (11, 3) Hz [38]. We include as well the effect of a residual quadratic light shift, which introduces a spin-dependent energy for the singly occupied sites  $qm_s^2$ . This shift may significantly handicap intersite spin-changing collisions. Interferometric measurements (see Supplemental Material, part S4 [37]) provide an upper value of 25 Hz for  $q/h$ . Singly occupied sites interact with each other through the Heisenberg-like interaction (2), where the coupling constants  $V_{ij}$  are evaluated taking into account the spatial extension of the on-site wave function, as discussed in the Supplemental Material, part S5 [37]. We have analyzed the exact quantum dynamics of the many-body system for a  $3 \times 3$  plaquette using exact diagonalization employing periodic boundary conditions. In order to evaluate the effect of the motion of residual holes left behind in the preparation process, we consider among the singly occupied sites one hole, initially localized at one site. We find that hopping, although not fully negligible, does not play a major role in our experiment, due to the rather strong lattice employed. As shown in Fig. 1 the results of the plaquette calculation for  $q/h \approx 15$  Hz are in very good agreement with our experimental data, confirming that the observed spin dynamics results from the XXZ spin-spin interactions in Eq. (3).

We now discuss the case where we do not empty doubly occupied sites (doublons). As shown below, this scenario is characterized by the rich interplay between contact interactions and DDI in the  $s = 3$  spin gas. The system consists of a core of doublons surrounded by a shell of singlons, following the ‘‘wedding cake’’ atomic distribution characteristic of a trapped Mott-insulator state [39]. We operate also in this case at a  $B$  field ( $\approx 10$  mG) much larger than the critical field for spontaneous demagnetization [30] that precludes any spin dynamics when atoms are prepared in  $m_s = -3$ . The state preparation at  $t = 0$  is identical to the singlon case, and the subsequent spin dynamics is illustrated in Figs. 1–3. At a short time scale, we observe fast

spin oscillations (Fig. 2), which damp in a few hundred  $\mu\text{s}$ . Then a second and slower dynamics occurs (Fig. 3), showing two to three spin oscillations with a period of about 3 ms. After these oscillations damp out, we observe a slow drift of populations similar to the case of singlons, as shown in Fig. 1. All the observed spin dynamics occurs at constant magnetization.

The fast spin oscillations shown in Fig. 2 result from on-site spin-dependent contact interactions. For an isolated site with two atoms, the eigenstates are characterized by a total spin  $S$  and spin projection  $M$  along the  $B$  field. A state of two atoms in  $m_s = -2$  in the same lattice site constitutes a linear superposition of states with  $M = -4$  and  $S = 6$  and  $4$ ,  $\sqrt{\frac{6}{11}}|6, -4\rangle - \sqrt{\frac{5}{11}}|4, -4\rangle$ . Thus a Rabi-like oscillation [40] is expected, with a period corresponding to the beating of the two eigenfrequencies:  $T_c = (\hbar/n_0|g_6 - g_4|)$ , where  $n_0 = \int d^3r |\psi_0(\mathbf{r})|^4$ , with  $\psi_0(\mathbf{r})$  the on-site wave function,  $g_s = 4\pi(\hbar^2/m)a_s$  [41],  $m$  the mass of the atoms and  $a_s$  the  $s$ -wave scattering length associated with the scattering channel with total spin  $S$ . For the data in Fig. 2,  $n_0 \approx 6.3 \times 10^{20} \text{ m}^{-3}$ . Employing the values of  $a_6$  and  $a_4$  from Ref. [42], we then obtain a theoretical oscillation period  $T_c \approx 320 \pm (50) \mu\text{s}$ , in good agreement with the period of the oscillations of the populations in  $m_s = -3, -2$  shown in Fig. 2, which is  $280 \pm (30) \mu\text{s}$ . These results constitute the first observation of spin exchange dynamics due to contact interactions in a  $s = 3$  spinor gas. Note that on-site spinor dynamics is much faster in

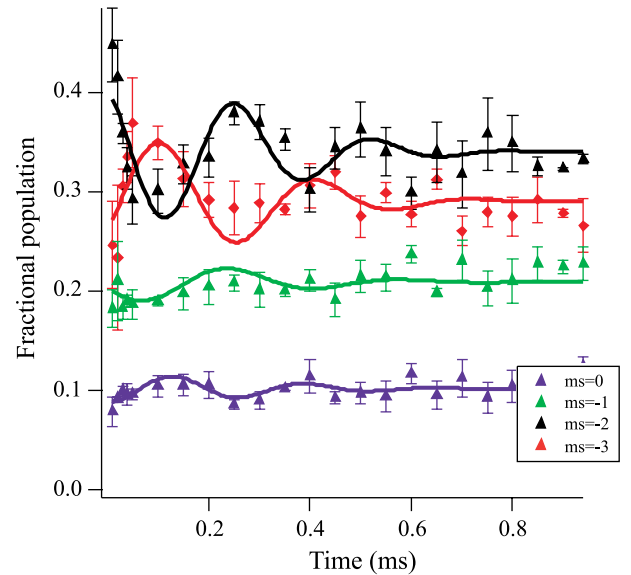


FIG. 2 (color online). Fast spin exchange dynamics due to contact interactions. The experimental evolution of the different spin components shows damped oscillations. For this specific data, the lattice depth was reduced, corresponding to lattice band gaps of  $(\omega_x^L, \omega_y^L, \omega_z^L) = 2\pi \times (100, 50, 145)$  kHz. The value of the pseudo period for  $m_s = -3, -2$  is in good agreement with theory. Full lines are results of fits with exponentially damped sinusoids.

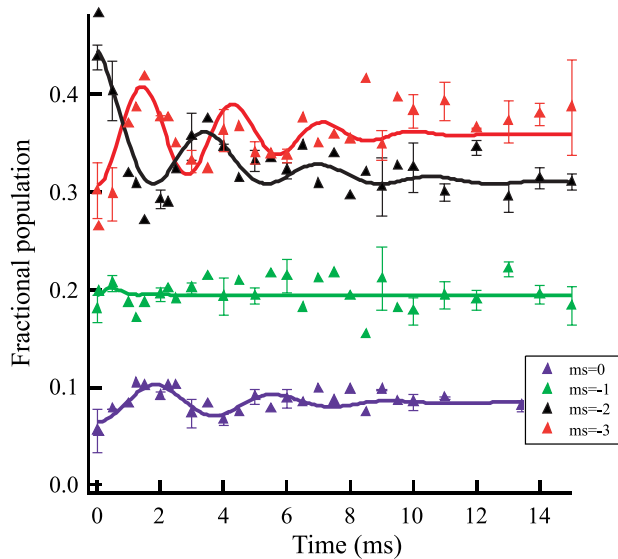


FIG. 3 (color online). Slow spin exchange dynamics due to dipole-dipole interactions. The experimental evolution of different spin components shows oscillations on a few ms time scale. Lines are results of fits with exponentially damped sinusoids.

chromium than in other spinor gases [40,43], due to the much larger difference between the scattering lengths of the relevant collision channels. We also observe a much stronger damping (of about 2 kHz) than in Refs. [40,43].

At longer time scales (see Fig. 3) the observed spin oscillations present a characteristic frequency much smaller than that of the short-time oscillations. To demonstrate that these ms-scale oscillations and in general the long-time spin dynamics result mostly from intersite DDIs, we have applied magnetic field gradients,  $\Delta B$ , to our sample. These gradients induce Zeeman energy shifts between adjacent sites. When these shifts are larger than the nonlocal interaction, intersite spin dynamics is energetically forbidden. We apply a few  $\text{G cm}^{-1}$  (note that  $1 \text{ G cm}^{-1}$  corresponds to a Zeeman shift of  $\Delta E = 70 \text{ Hz}$  between two adjacent sites in our lattice). The energy shifts associated with the magnetic field gradient lie below the excitation gap for the Mott-insulator state [36]. We observe (see Supplemental Material, part S6 [37]) strong suppression of the spin dynamics amplitude in the presence of gradients, which shows that the spin dynamics involves a nonlocal coupling between atoms. The value of  $\Delta B$  at which the amplitudes significantly drop corresponds to  $\Delta E/h$  of the same order as the frequency of the oscillations shown in Fig. 3.

Hence, spin dynamics at  $t > 1 \text{ ms}$  results mostly from intersite DDIs. Moreover, as shown in Fig. 1, spin oscillations at the ms time scale disappear when doublons are removed. These observations provide a strong evidence that the long-time spin oscillations are due to intersite DDIs between doubly occupied sites. Note that, interestingly, doubly occupied sites lead to stronger DDIs compared to single  $^{52}\text{Cr}$  atoms, as pairs of atoms behave like molecular  $\text{Cr}_2$  magnets with larger magnetic moments,

without the actual need to create the molecules using Feshbach resonances.

To qualitatively account for the role of the DDIs between doublons in the long-time spin oscillations, we have developed a toy model consisting of two doubly occupied sites. Twelve possible states may be dynamically reached via intersite DDIs for a preserved total magnetization  $M_t = -8$ . We show in the Supplemental Material, part S7 [37] that the total spin  $S$  of a pair of particles in one site is not modified by the interaction with other sites, which confirms that pairs of particles do behave like large spins  $S$  interacting through long range DDIs. Starting with an initial state  $|S = 6, M = -4\rangle$  in both sites, our model qualitatively reproduces the shape of the oscillations shown in Fig. 3 (see Supplemental Material, part S7 [37]). Nevertheless this toy model cannot reproduce the observed time scale for the oscillations, as it only includes the interactions between two sites, while each site is in fact coupled to many sites due to the long range character of DDIs. Our experiment shows that the frequency of the spin oscillations is about 7 times faster than that predicted by the two-site model (and still 2.5 faster if the coupling of one site to its neighbors is described by an effective coordination number, see part S7 in [37]). This indicates that a much more elaborate many-body theoretical treatment would be necessary to interpret this intriguing spin dynamics, with an interplay between short-range physics and long-range interactions between many sites.

In conclusion, we have obtained strong evidence of intersite spin exchange in a dipolar quantum gas due to the long-range character of the dipole-dipole interactions [44]. Dipole-induced spin exchange, being much larger than that resulting from superexchange in nondipolar gases in deep optical lattices, opens fascinating perspectives for the study of quantum magnetism with magnetic atoms. We have in particular shown that a chromium lattice gas with maximally one atom per site exhibits purely intersite spin exchange, realizing a lattice model resembling the  $t$ - $J$  model of strongly correlated electrons. We have studied in addition spinor dynamics resulting from doubly occupied sites, which stems from the interplay between spin-dependent contact and dipole-dipole interactions. We have shown in particular that fast short-time spin oscillations result from spin-changing contact interactions, constituting the first observation of these interactions in a  $s = 3$  gas. By contrast, we have demonstrated that longer-time coherent spin oscillations are the result of intersite spin exchange between doubly occupied sites. Our experiment demonstrates hence not only the potential of dipolar gases for quantum simulation of lattice models, but also the intriguing physics associated with lattice gases of large spin.

We acknowledge financial support from Conseil Régional d'Ile-de-France and from Ministère de l'Enseignement Supérieur et de la Recherche within IFRAF and CPER. L. S. acknowledges support from the

Deutsche Forschungsgemeinschaft (SA1031/6) and the Cluster of Excellence QUEST.

*Note added.*—Recently, we became aware of a recent work by the group of D. Jin and J. Ye, reporting on the observation of intersite DDIs between pairs of dipolar heteronuclear molecules trapped in an optical lattice, at low filling factors [44].

\*Corresponding author.

laurent.vernac@univ-paris13.fr

- [1] A. Auerbach, *Interacting Electrons and Quantum Magnetism* (Springer-Verlag, New York, 1994).
- [2] I. Bloch, J. Dalibard, and W. Zwerger, *Rev. Mod. Phys.* **80**, 885 (2008).
- [3] I. Bloch, J. Dalibard, and S. Nascimbene, *Nat. Phys.* **8**, 267 (2012).
- [4] Y. Kawaguchi and M. Ueda, *Phys. Rep.* **520**, 253 (2012).
- [5] D. Stamper-Kurn and M. Ueda, *Rev. Mod. Phys.* **85**, 1191 (2013).
- [6] A. Imambekov, M. Lukin, and E. Demler, *Phys. Rev. A* **68**, 063602 (2003).
- [7] A. Rapp, G. Zarand, C. Honerkamp, and W. Hofstetter, *Phys. Rev. Lett.* **98**, 160405 (2007).
- [8] M. Hermele, V. Gurarie, and A. M. Rey, *Phys. Rev. Lett.* **103**, 135301 (2009).
- [9] A. Griesmaier, J. Werner, S. Hensler, J. Stuhler, and T. Pfau, *Phys. Rev. Lett.* **94**, 160401 (2005).
- [10] Q. Beaufils, R. Chicireanu, T. Zanon, B. Laburthe-Tolra, E. Maréchal, L. Vernac, J.-C. Keller, and O. Gorceix, *Phys. Rev. A* **77**, 061601(R) (2008).
- [11] M. Lu, N. Q. Burdick, S. H. Youn, and B. L. Lev, *Phys. Rev. Lett.* **107**, 190401 (2011).
- [12] M. Lu, N. Q. Burdick, and B. L. Lev, *Phys. Rev. Lett.* **108**, 215301 (2012).
- [13] K. Aikawa, A. Frisch, M. Mark, S. Baier, A. Rietzler, R. Grimm, and F. Ferlaino, *Phys. Rev. Lett.* **108**, 210401 (2012).
- [14] K.-K. Ni, S. Ospelkaus, M. H. G. de Miranda, A. Pe'er, B. Neyenhuis, J. J. Zirbel, S. Kotochigova, P. S. Julienne, D. S. Jin, and J. Ye, *Science* **322**, 231 (2008).
- [15] A. Chotia, B. Neyenhuis, S. A. Moses, B. Yan, J. P. Covey, M. Foss-Feig, A. M. Rey, D. S. Jin, and J. Ye, *Phys. Rev. Lett.* **108**, 080405 (2012).
- [16] C. H. Wu, J. W. Park, P. Ahmadi, S. Will, and M. W. Zwierlein, *Phys. Rev. Lett.* **109**, 085301 (2012).
- [17] M. S. Heo, T. T. Wang, C. A. Christensen, T. M. Rvachov, D. A. Cotta, J. H. Choi, Y. R. Lee, and W. Ketterle, *Phys. Rev. A* **86**, 021602(R) (2012).
- [18] R. Barnett, D. Petrov, M. Lukin, and E. Demler, *Phys. Rev. Lett.* **96**, 190401 (2006).
- [19] A. Micheli, G. K. Brennen, and P. Zoller, *Nat. Phys.* **2**, 341 (2006).
- [20] A. V. Gorshkov, S. R. Manmana, G. Chen, J. Ye, E. Demler, M. D. Lukin, and A. M. Rey, *Phys. Rev. Lett.* **107**, 115301 (2011).
- [21] D. Peter, S. Muller, S. Wessel, and H. P. Buchler, *Phys. Rev. Lett.* **109**, 025303 (2012).
- [22] M. L. Wall, K. Maeda, and L. D. Carr, [arXiv:1305.1236](https://arxiv.org/abs/1305.1236) [Ann. Phys. (N.Y.) (to be published)].
- [23] M. A. Baranov, M. Dalmonte, G. Pupillo, and P. Zoller, *Chem. Rev.* **112**, 5012 (2012).
- [24] M. Anderlini, P. J. Lee, B. L. Brown, J. Sebby-Strabley, W. D. Phillips, and J. V. Porto, *Nature (London)* **448**, 452 (2007).
- [25] S. Trotzky, P. Cheinet, S. Folling, M. Feld, U. Schnorrberger, A. M. Rey, A. Polkovnikov, E. A. Demler, M. D. Lukin, and I. Bloch, *Science* **319**, 295 (2008).
- [26] J. Simon, W. S. Bakr, R. Ma, M. E. Tai, P. M. Preiss, and M. Greiner, *Nature (London)* **472**, 307 (2011).
- [27] F. Meinert, M. J. Mark, E. Kirilov, K. Lauber, P. Weinmann, A. J. Daley, and H.-C. Nägerl, *Phys. Rev. Lett.* **111**, 053003 (2013).
- [28] M. Fattori, G. Roati, B. Deissler, C. D'Errico, M. Zaccanti, M. Jona-Lasinio, L. Santos, M. Inguscio, and G. Modugno, *Phys. Rev. Lett.* **101**, 190405 (2008).
- [29] S. Müller, J. Billy, E. A. L. Henn, H. Kadau, A. Griesmaier, M. Jona-Lasinio, L. Santos, and T. Pfau, *Phys. Rev. A* **84**, 053601 (2011).
- [30] B. Pasquiou, E. Maréchal, G. Bismut, P. Pedri, L. Vernac, O. Gorceix, and B. Laburthe-Tolra, *Phys. Rev. Lett.* **106**, 255303 (2011).
- [31] Y. Kawaguchi, H. Saito, and M. Ueda, *Phys. Rev. Lett.* **96**, 080405 (2006).
- [32] B. Pasquiou, G. Bismut, E. Maréchal, P. Pedri, L. Vernac, O. Gorceix, and B. Laburthe-Tolra, *Phys. Rev. Lett.* **106**, 015301 (2011).
- [33] A. de Paz, A. Chotia, E. Maréchal, P. Pedri, L. Vernac, O. Gorceix, and B. Laburthe-Tolra, *Phys. Rev. A* **87**, 051609 (R) (2013).
- [34] S. Hensler, J. Werner, A. Griesmaier, P. O. Schmidt, A. Görlitz, T. Pfau, S. Giovanazzi, K. Rzażewski, *Appl. Phys. B* **77**, 765 (2003).
- [35] P. L. Gould, G. A. Ruff, and D. E. Pritchard, *Phys. Rev. Lett.* **56**, 827 (1986).
- [36] M. Greiner, O. Mandel, T. Esslinger, T. W. Hansch, and I. Bloch, *Nature (London)* **415**, 39 (2001).
- [37] See Supplemental Material at <http://link.aps.org/supplemental/10.1103/PhysRevLett.111.185305> for details about the preparation of the Mott State, the preparation in the  $m_s = -2$  state, the suppression of multiply-occupied sites using dipolar relaxation, the measurement of the quadratic light shift with interferometry, the plaquette simulation for singlons, the effect of a magnetic gradient during the spin evolution, and the two-site model for the spin dynamics of doubly-occupied sites.
- [38] W. Zwerger, *J. Opt. B* **5**, S9 (2003).
- [39] B. DeMarco, C. Lannert, S. Vishveshwara, and T. C. Wei, *Phys. Rev. A* **71**, 063601 (2005).
- [40] A. Widera, F. Gerbier, S. Folling, T. Gericke, O. Mandel, and I. Bloch, *Phys. Rev. Lett.* **95**, 190405 (2005).
- [41] L. Pitaevskii and S. Stringari, *Bose-Einstein Condensation* (Oxford University Press, Oxford, 2003).
- [42] B. Pasquiou, G. Bismut, Q. Beaufils, A. Crubellier, E. Maréchal, P. Pedri, L. Vernac, O. Gorceix, and B. Laburthe-Tolra, *Phys. Rev. A* **81**, 042716 (2010).
- [43] J. S. Krauser, J. Heinze, N. Fläschner, S. Götze, O. Jürgensen, D.-S. Lühmann, C. Becker, and K. Sengstock, *Nat. Phys.* **8**, 813 (2012).
- [44] B. Yan, S. A. Moses, B. Gadway, J. P. Covey, K. R. A. Hazzard, A. M. Rey, D. S. Jin, and J. Ye, *Nature (London)* **501**, 521 (2013).